Influence of Timing Offset in Multiband OFDM Systems

X. Yuan, J. Zhang, D. Jayalath and T. Abhayapala

Wireless Signal Processing
National ICT Australia
Email: eric.yuan@rsise.anu.edu.au

ABSTRACT

In Cyclix Prefix OFDM (CP) systems, synchronization to the maximal multipath signal generally causes no problem, however, inter carrier interference (ICI) will be introduced in Zero-padding OFDM (ZP-OFDM) systems, e.g, multiband OFDM UWB (MB-OFDM) systems. In this paper, based on the overlap-and-add (ZP-OFDM-OLA) method typically applied in MB-OFDM, we analyze the cause of the ICI and the performance degradation due to the ICI. The expressions of the channel estimation error, signal-to-noise ratio and ICI are derived. Simulation results are also provided, which show good match with the theoretical results.

I. INTRODUCTION

Multiband OFDM UWB (MB-OFDM) system is the official specification of the Wimedia/MBOA association, and is being considered as one of the short-range high-speed WPAN standards. One of the main difference between MB-OFDM and popular OFDM systems, e.g., WLAN, is that the cyclic prefix (CP) in the latter is replaced by the zero-padding (ZP) in the former. The introduction of ZP is to reduce the power consumption and spectrum ripple, which is very important for a power spectrum density limited system such as MB-OFDM. However, ZP-OFDM leads to some different problems in the system design compared to CP-OFDM, especially in channel estimation and equalization. These problems are generally associated with synchronization or timing.

In MB-OFDM systems, synchronization, including packet sync and frame sync, is generally realized by calculating the correlation between the training symbols and local sequences [1]. The time according to the peaky output is generally chosen as the sync point. Considering a frequency selective channel model, this sync point actually corresponds to the arrival time of the maximal multipath. In CP-OFDM systems, sync to the strongest multipath does not cause any trouble, however, in ZP-OFDM, this type of synchronization will lead to performance degradation, unless some remediation is adopted.

OFDM is very sensitive to the timing error and the frequency error [2], [3], [4]. These issues have been well addressed in the literature for CP-OFDM systems, however, the related research for ZP-OFDM is much lesser. In [5], the inter-carrier interference (ICI) and bit error rate (BER) is analyzed for ZP-OFDM systems, but the frequency samples in the receiver is generated in a way similar to CP-OFDM, without considering the special method applied in ZP-OFDM systems. As shown in [6], there are different methods to generate frequency samples and to implement equalization. The common approach with lower complexity is called overlap-and-add (OLA), which is feasible for practical implementation.

In this paper, we analyze the effect of timing offset based on the OLA method. The performance degradation associated with this timing offset, including the channel estimation accuracy, ICI and BER, is investigated using IEEE802.15.3a [7] channel models. The following part of this paper is organized as follows. In Section II, ZP-OFDM system model is introduced, and signal processing is formulated. In Section III, the effects of timing offset is derived theoretically. In Section IV, the simulation result in given. Section V gives the conclusions.

II. SYSTEM MODEL

A. ZP-OFDM Model

As shown in Fig.1, the ith $N \times 1$ information block $\mathbf{s}_N^{(i)}$ with normalized power is first multiplexed by an

National ICT Australia is funded by the Australian Government's Department of Communications, Information Technology and the Arts and the Australian Research Council through Backing Australia's Ability and the ICT Centre of Excellence program.

X. Yuan, J. Zhang, D. Jayalath and T. Abhayapala are also with the Department of Information Engineering, Australian National University.

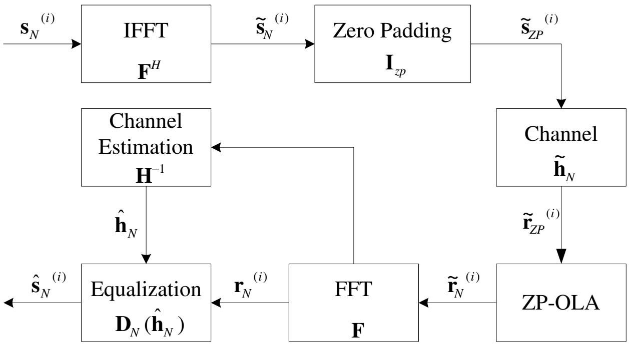

Fig. 1. ZP-OFDM-OLA baseband processing diagram.

IFFT matrix $\mathbf{F}^{-1}$ to transfer to time domain signal $\tilde{\mathbf{s}}_N^{(i)}$($\tilde{\cdot}$ means the corresponding signal is in time domain throughout this paper), where $\mathbf{F}$ with (k,n)th entry $= \exp(-j2\pi kn/N)/\sqrt{N}$ and $\mathbf{F}^{-1} = \mathbf{F}^{\mathcal{H}}$, $(\cdot)^{\mathcal{H}}$ denoting conjugate transpose. A zero sequence of length N_{zp} is then appended to the end of each $\tilde{\mathbf{s}}_N^{(i)}$ to yield $P \times 1$ transmitted time domain block $\tilde{\mathbf{s}}_{zp}^{(i)} = \mathbf{I}_{zp}\mathbf{F}_N\mathbf{s}_N^{(i)}$, where $P = N + N_{zp}$, $\mathbf{I}_{zp} = [\mathbf{I}_N 0]^{\mathcal{H}}$, and $\mathbf{I}_N$ is the unit matrix with dimension of N. The frequency-selective channel model can be modelled as a FIR filter with time domain impulse response vector $\tilde{\mathbf{h}}_N = [\tilde{h}_0, \tilde{h}_1, \ldots, \tilde{h}_L, 0, \ldots, 0]^T$, L is the channel order. The received symbol signal is given by

$$
\begin{aligned}
\tilde{\mathbf{r}}_{zp}^{(i)} &= \mathbf{H}\mathbf{F}_{zp}\mathbf{s}_N^{(i)} + \mathbf{H}_{IBI}\mathbf{F}_{zp}\mathbf{s}_N^{(i-1)} + \tilde{\mathbf{n}}_p^{(i)} \\
&= \mathbf{H}\mathbf{F}_{zp}\mathbf{s}_N^{(i)} + \tilde{\mathbf{n}}_p^{(i)} \\
&= \mathbf{H}_0\mathbf{F}_N^{\mathcal{H}}\mathbf{s}_N^{(i)} + \tilde{\mathbf{n}}_p^{(i)}
\end{aligned} \tag{1}
$$

where $\mathbf{H}$ is the $P \times P$ lower triangle Toeplitz matrix with the first column $[h_0, h_1, \ldots, h_L, 0, \ldots, 0]^T$, and $\mathbf{H}_{IBI}$ is a $(N + N_{zp}) \times (N + N_{zp})$ upper triangular Toeplitz matrix with the first row $[0, \ldots, 0, h_L, \ldots, h_1]$, and $\mathbf{F}_{zp} = [\mathbf{F}_N 0]^{\mathcal{H}}$. The channel order L satisfies $L \leq N_{zp}$. The matrix $\mathbf{H}_0$ is a $(N+N_{zp})\times N$ full-rank Toeplitz matrix and is always guaranteed to be invertible. A straightforward method for equalization is to calculate the pseudo-inverse of $\mathbf{H}_0$, and the equalizer becomes $\mathbf{G}_{zf} = (\mathbf{H}_0\mathbf{F}^{\mathcal{H}})^\dagger = \mathbf{F}\mathbf{H}_0^\dagger$, where $\dagger$ denotes pseudo-inverse of a matrix. The equalized symbol vector at the receiver is given by $\hat{\mathbf{s}}_N^{(i)} = \mathbf{G}_{zf}\tilde{\mathbf{r}}_{zp}^{(i)} = \mathbf{s}_N^{(i)} + \mathbf{F}\mathbf{H}_0^\dagger\mathbf{n}_p(i)$.

B. ZP-OFDM-OLA Method

The above method is capable of equalization even when the channel has null frequency coefficients. However, the complexity associated with calculating a pseudo-inverse of a large matrix is very high. To avoid computing the pseudo-inversion of a matrix, some sub-optimal equalization schemes are developed [6]. From the practical point of view, ZP-OFDM-OLA is optimal in the case of ideal synchronization, and has complexity similar to that applied in CP-OFDM. Here, ideal synchronization refers to the situation when the sync point corresponds to the first arrival multipath rather than the maximal one. Similar to CP-OFDM, channel invertibility with null response is not guaranteed anymore.

In ZP-OFDM-OLA method, the time domain samples in the guarding interval are added to the samples from the beginning of the FFT window. The concrete algorithm for ZP-OFDM-OLA can be found in [6]. FFT is then applied to the combined output. With ideal synchronization, the received signal after ZP-OFDM-OLA and FFT processing is given by

$$
\begin{aligned}
\mathbf{r}_N^{(i)} &= \mathbf{F}_N\tilde{\mathbf{r}}_N^{(i)}(0) \\
&= \mathbf{D}_N(\mathbf{h}_N)\mathbf{s}_N^{(i)} + \mathbf{n}_N^{(i)}
\end{aligned} \tag{2}
$$

where $\tilde{\mathbf{r}}_N^{(i)}(0) = [\tilde{r}^{(i)}(0) \quad \tilde{r}^{(i)}(1)\ldots\tilde{r}^{(i)}(N-1)]^T$, $\mathbf{h}_N = \mathbf{FFT}(\tilde{\mathbf{h}}_N)$, $\mathbf{D}_N(\mathbf{h}_N)$ denotes the $N \times N$ diagonal matrix with $\mathbf{h}_N$ on its diagonal entry, and $\mathbf{n}_N^{(i)} = \mathbf{F}_N\tilde{\mathbf{n}}_N^{(i)} \sim \mathcal{N}(0, \sigma^2)$, and the estimated information $\hat{\mathbf{s}}_N^{(i)}$ can be given as follows:

$$
\hat{\mathbf{s}}_N^{(i)} = \mathbf{D}_N^\dagger(\mathbf{h}_N)\mathbf{r}_N^{(i)} \tag{3}
$$

where $\hat{\mathbf{s}}_N^{(i)} = [\hat{s}^{(i)}(0) \quad \hat{s}^{(i)}(1)\ldots\hat{s}^{(i)}(k)\ldots\hat{s}^{(i)}(N-1)]^T$ is the estimation of $\mathbf{s}_N^{(i)}(k)$ which is the kth OFDM symbol of $\mathbf{s}_N^{(i)}$.

III. Analysis of Timing Error

In the presence of timing error, assume the block timing error is d-samples , the d-shift version of $\tilde{\mathbf{r}}_N^{(i)}(0)$, $\tilde{\mathbf{r}}_N^{(i)}(d)$, becomes $\tilde{\mathbf{r}}_N^{(i)}(d) = [\tilde{r}^{(i)}(d) \quad \tilde{r}^{(i)}(d+1)\ldots\tilde{r}^{(i)}(N)\ldots\tilde{r}(N+d-1)]^T$. The equation (2) then becomes

$$
\begin{aligned}
\mathbf{r}_N^{(i)} &= \mathbf{F}_N\tilde{\mathbf{r}}_N^{(i)}(d) \\
&= \mathbf{D}_N(\mathbf{h}_N^{(i)}(d))\mathbf{s}_N^{(i)} - \mathbf{F}_N\mathbf{T}_N(\tilde{\mathbf{h}}_N^{(i)}(-d))\mathbf{F}_N^{\mathcal{H}}\mathbf{s}_N^{(i)} \\
&+ \mathbf{n}_N^{(i)}
\end{aligned} \tag{4}
$$

where $\mathbf{h}_N^T(d) = \mathbf{FFT}(\tilde{h}_d \quad \tilde{h}_{d+1}\ldots\tilde{h}_{N-1} \quad \tilde{h}_0\ldots\tilde{h}_{d-1})$, $\tilde{\mathbf{h}}_N(-d) = [0\ldots\tilde{h}_0 \quad \tilde{h}_1\ldots\tilde{h}_{d-1}]^T$, and $\mathbf{T}_N(\mathbf{h}_N)$is a Toeplitz matrix with first column given by $\mathbf{h}_N$.

Assume $\mathbf{r}_N^{(i)} = [r^{(i)}(0) \quad r^{(i)}(1)\ldots r^{(i)}(k)\ldots r^{(i)}(N-1)]^T$, the obtained signal $r^{(i)}(k)$ contains ICI, and can be expressed as

$$
\begin{aligned}
r^{(i)}(k) &= s^{(i)}(k)\sum_{\ell=0}^{L-1}\tilde{h}_\ell^{(i)} I_{k,k}(d-\tau_\ell^{(i)}) \\
&+ \sum_{m=0,m\neq k}^{N-1} s^{(i)}(m)\sum_{\ell=0}^{L-1}\tilde{h}_\ell^{(i)} I_{m,k}(d-\tau_\ell^{(i)}) \\
&+ n^{(i)}(k)
\end{aligned} \tag{5}
$$

where $\tilde{h}^{(i)}(n)=\sum_{\ell=0}^{L-1}\tilde{h}_\ell^{(i)}\delta(n-\tau_\ell^{(i)})$, $\tau_\ell^{(i)}$ is the delay of ℓth path, $I_{k,k}(\cdot)$ and $I_{m,k}(\cdot)$ denote the useful signal and ICI, respectively, and they have different expressions under different conditions.

When $d'=(d-\tau_\ell^{(i)})>0$, we have

$$
\begin{aligned}
I_{k,k}(d') &= \tfrac{1}{N}(N-d')e^{j2\pi kd'/N} \\
I_{m,k}(d') &= -\frac{d'}{N}\frac{\mathrm{sinc}[\frac{\pi}{N}(m-k)d']}{\mathrm{sinc}\frac{\pi}{N}(m-k)}e^{j\phi_{m,k}(d')},
\end{aligned} \tag{6}
$$

and

$$
\phi_{m,k}(d')=\frac{\pi}{N}[2kd'+(d'-1)(m-k)]. \tag{7}
$$

When $-N_{zp}\le d'=(d-\tau_\ell^{(i)})\le 0$, we have

$$
\begin{aligned}
I_{k,k}(d') &= e^{j2\pi kd'/N} \\
I_{m,k}(d') &= -\frac{d'}{N}\frac{\mathrm{sinc}[\frac{\pi}{N}(m-k)d']}{\mathrm{sinc}[\frac{\pi}{N}(m-k)]}e^{j\phi^{(1)}_{m,k}(d')} \\
&- \frac{(N-d')}{N}\frac{\mathrm{sinc}[\frac{\pi}{N}(m-k)(N-d')]}{\mathrm{sinc}[\frac{\pi}{N}(m-k)]}e^{j\phi^{(2)}_{m,k}(d')} \\
&= 0 \quad (\mathbf{if}(k\neq m)),
\end{aligned} \tag{8}
$$

$$
\begin{aligned}
\phi^{(1)}_{m,k}(d') &= \tfrac{\pi}{N}[-2kd'-(d'+1)(m-k)] \\
\phi^{(2)}_{m,k}(d') &= \tfrac{\pi}{N}[2k(N-d')+(N-d'-1)(m-k)].
\end{aligned}
$$

When $d'=(d-\tau_\ell^{(i)})\le -N_{zp}$, the ICI will be produced and we will have an equation similar to (5). ICI introduced can be expressed by $I_{m,k}(\cdot)$ and is a function of d'.

Thus, from (8), it is obvious that limited multipath will contribute to the ICI due to the process of ZP-OFDM-OLA in the absence of frequency offset. When N is large, the ICI in (5) will be normal distributed according to the central limit theorem, and have zero mean. Define the signal-to-interference-ratio (SIR) as

$$
\mathrm{SIR}=10\log(\frac{\sigma_s}{\sigma_{ICI}}) \tag{9}
$$

where σ_{ICI} and σ_s are power of interference and signal respectively, given by

$$
\sigma_{ICI} = \sum_{m=0,m\neq k}^{N-1}\sum_{\ell=0}^{\ell_d}E\{|\tilde{h}_\ell|^2\}|I_{m,k}(d-\tau_\ell)|^2 \tag{10}
$$

$$
\sigma_s = \sum_{\ell=0}^{\ell_d}E\{|\tilde{h}_\ell|^2\}(1-\frac{(d-\tau_\ell)}{N})^2+\sum_{\ell=\ell_d+1}^{L}E\{|\tilde{h}_\ell|^2\} \tag{11}
$$

where $\ell_d=\arg\max_\ell(\tau_\ell\le d)$ and the channel coefficients are normalized.

The signal to interference and noise ratio(SINR) γ can be derived from (5), (10) and (11), and the theoretical relationship of OFDM between BER and average γ with multipath channel can be given [8] as

$$
BER=\tfrac{1}{2}\big(1-\tfrac{1}{\sqrt{1+\frac{1}{\gamma}}}\big). \tag{12}
$$

Since channel estimation also contains errors due to timing error, this needs to be taken into consideration when evaluating the BER performance of detection. When training based channel estimation is used, the channel response can be derived from equations (5), (6), (7), and (8). Let $\hat{h}_k$ be the kth element of $\hat{\mathbf{h}}$ which is the estimated channel response in frequency domain, and let $s^{(p)}(k)$ be the kth element of $\mathbf{s}^{(\mathbf{p})}$ which is the training symbol, we have

$$
\begin{aligned}
\hat{h}(k) &= h(k)-s^{(p)*}(k)\sum_{\ell=0}^{\ell_d}\tilde{h}_\ell\sum_{m=0}^{N-1}s^{(p)}(m)I_{m,k}(d-\tau_\ell) \\
&+ n(k) \\
&= h(k)-h_e(k)
\end{aligned} \tag{13}
$$

where $h_e(k)$ denotes the error of estimates.

The channel equalization can then be written as

$$
\begin{aligned}
\hat{s}(k) &= \frac{\hat{h}^*(k)}{|\hat{h}(k)|^2}\{h(k)s(k) \\
&- \sum_{\ell=0}^{\ell_d}\tilde{h}_\ell\sum_{m=0}^{N-1}s(m)I_{m,k}(d-\tau_\ell)+n(k)\} \\
&= s(k)+s_e(k)
\end{aligned} \tag{14}
$$

where $s_e(k)$ denotes the error of the detected symbols. According to the Central Limit Theorem, $s_e(k)$ can be approximated as a Gaussian variable assuming channel coefficients and symbols are random variables. It is straightforward that $s_e(k)$ has zero mean, and the variance of $s_e(k)$ is derived in Appendix and given by

$$
E[s_e(k)s_e^*(k)] \overset{\triangle=m-k}{=} 2\sum_{\ell=0}^{\ell_d}E\{|\tilde{h}_\ell|^2\}\sum_{\triangle=1}^{N-1}|I_\triangle(d-\tau_\ell)|^2+\sigma^2. \tag{15}
$$

Number of Data Subcarriers	100
Number of Pilot Carriers	12
Number of Guard Carriers	10
FFT windows	128
Zero-Padding samples	37

TABLE I
SYSTEM PARAMETERS USED IN THE SIMULATION.

Mode Characteristics	CM1	CM2	CM3	CM4
Mean Excess Delay(nsec)	5.0	9.9	15.9	30.1
RMS Delay (nsec)	5	8	15	25
NP(10dB)	12.5	15.3	24.9	41.2
NP (85%)	20.8	33.9	64.7	123.3
Energy Mean (dB)	-0.4	-0.5	0.0	0.3
Channel Energy (dB)	2.9	3.1	3.1	2.7

TABLE II
PARAMETERS OF CHANNEL MODEL.

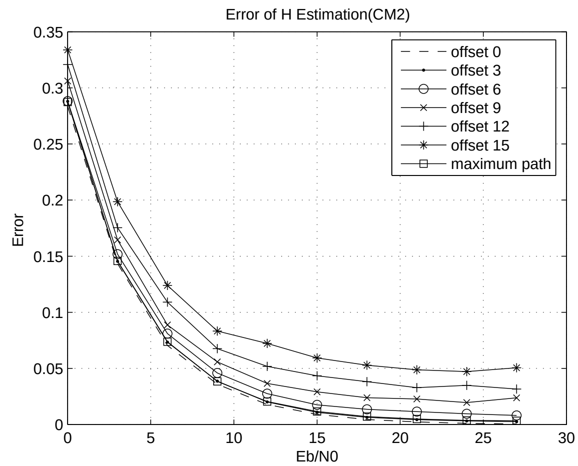

Fig. 2. Mean squared error of channel estimates in CM2.

IV. SIMULATIONS

The simulation platform is setup following the signal format and the channel model [9] in the specification of MB-OFDM system. Main parameters adopted are shown in Table I and Table II.

We assume that the channel is stable during one MB-OFDM packet period and AWGN is present. The channel coefficients are normalized so that the power of the channel impulse response equals one. As discussed before, channel estimates contain ICI errors. Fig. 2 shows an example of how the mean squared error (MSE) of the channel estimates varies with the sync point and SNR in CM2. The value of offset refers to the distance between the current sync point and the starting of the channel. It is obvious that basically the MSE of channel estimates increases with the offset.

Figs. 3-6 show the BER for different timing offset when equalization is implemented with estimated channel coefficients in channel CM1, CM2, CM3 and CM4. In these figures, the maximum path refers to the case when the maximum multipath is selected as the sync point, which is the general rule in system implementation. From the figures, two conclusions can be derived:

1) The BER performance generally decreases with increasing the offset. However, when channel has a much larger delay than the guarding interval as in CM3 and CM4, this changes as multipath signals with larger energy are widely separated.
2) Selecting maximal multipath (peak output) in synchronization process is generally a good option in small spread channel such as CM1 and CM2, however, new schemes are necessary for large spread channel such as CM3 and CM4.

V. CONCLUSIONS

In this paper, we have analyzed the impact of timing offset on the performance of ZP-OFDM system in both theoretical and simulation approach. It is demonstrated that the performance has notable degradation in the presence of timing offset, and the strategy of synchronizing to the maximal multipath does not promise best performance. The degree of the ICI introduced due to the timing offset depends on the channel model, or more specifically, on the length of channel delay spread and the distribution of multipath energy. These findings motivate the design of new synchronization algorithms.

APPENDIX

The error term $s_e(k)$ can be written as

$$\begin{aligned} s_e(k) &= \frac{\hat{h}^*(k)}{|\hat{h}(k)|^2}\{h_e(k)s(k) \\ &- \textstyle\sum_{\ell=0}^{\ell_d}\tilde{h}_\ell\sum_{m=0}^{N-1}s(m)I_{m,k}(d-\tau_\ell)+n(k)\} \\ &= \frac{\hat{h}^*(k)}{|\hat{h}(k)|^2}\sum_{m=0}^{N-1}\{s^{(p)*}(k)s(k)s^{(p)}(m)-s(m)\} \\ &\times \sum_{\ell=0}^{\ell_d}\tilde{h}_l I_{m,k}(d-\tau_\ell)+n^{'}(k). \end{aligned}$$

By assuming statistical independence among $s(k), s^{(p)}(k), \tilde{h}_\ell$ and $n(k)$, then we have

$$\begin{aligned} E[s_e(k)s_e^*(k)] &= 2\sum_{\ell=0}^{\ell_d}|\tilde{h}_l|^2\sum_{m=0,m\neq k}^{N-1}|I_{m,k}(d-\tau_\ell)|^2+\sigma^2 \\ &\overset{\triangle=m-k}{=} 2\sum_{\ell=0}^{\ell_d}E\{|\tilde{h}_\ell|^2\}\sum_{\triangle=-k,\triangle\neq 0}^{N-k-1}|I_\triangle(d-\tau_\ell)|^2+\sigma^2. \end{aligned}$$

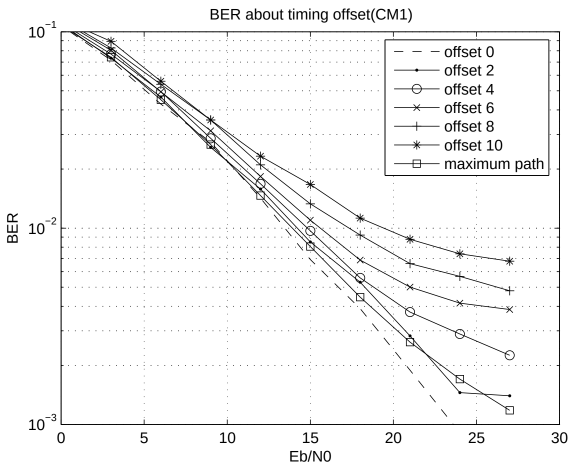

Fig. 3. BER based on estimated channel equalization(CM1)

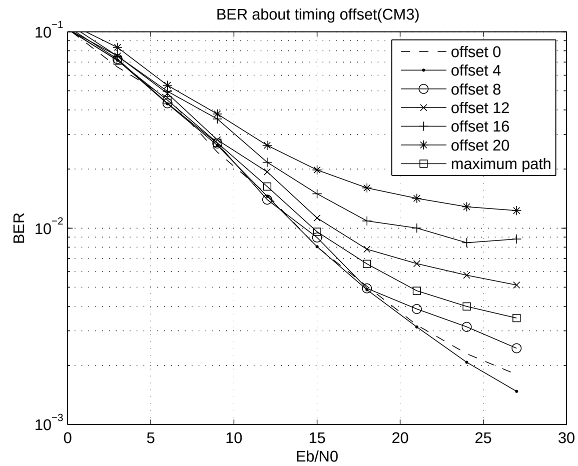

Fig. 5. BER based on estimated channel equalization(CM3)

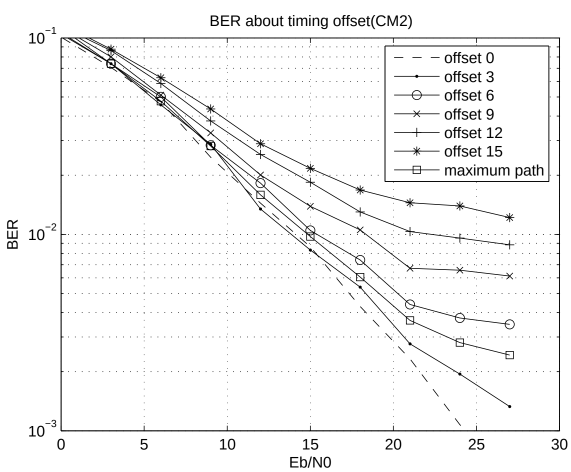

Fig. 4. BER based on estimated channel equalization(CM2)

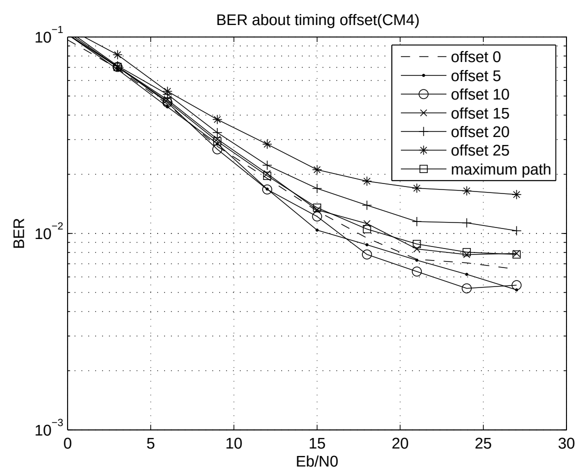

Fig. 6. BER based on estimated channel equalization(CM4)

Note that $|I_\triangle(d)|^2 = |I_{N-\triangle}(d)|^2$, then

$$
\begin{aligned}
E[s_e(k)s_e^*(k)] &= 2\sum_{\ell=0}^{\ell_d} E\{|\tilde{h}_\ell|^2\} \sum_{\triangle=1}^{N-1} |I_\triangle(d-\tau_\ell)|^2 \\
&+ \sigma^2.
\end{aligned}
$$

REFERENCES

[1] A. Batra, J. Balakrishnan, G. R. Aiello, J. R. Foerster, and A. Dabak, "Design of a multiband ofdm system for realistic uwb channel environments," *IEEE Trans. Microw. Theory Tech*, vol. 52, no.9.

[2] T. Pollet and M. Moeneclaey, "Synchronizability of OFDM Signals," *Proc.Globecom*, vol. 3, pp. 2054–2058, Nov. 1995.

[3] T. Pollet, M. van Bladel, and M. Moeneclaey, "Ber Sensitivity of OFDM Systems to Carrier Frequency Offset and Wiener Phase Noise," *IEEE Trans. Commun.*, vol. 43, pp. 191–193, Feb./Mar./Apr. 1995.

[4] A.R.S.Bahai and B.R.Saltzberg, "Multi-carrier digital communciations theory and application of ofdm," *Kluwer Academic/Plenum Publisher*.

[5] C. Athaudage and R. Angiras, "Sensitivity of FFT-Equalized Zero-padded OFDM Systems to Time and Frequency Synchronization Errors," *The 16th Annual IEEE International Symposium on Personal Indoors and Mobile Radio Communications*, 2005.

[6] B. Muquet, Z. Wang, G. B. Giannakis, M. D. Courville, and P.Duhamel, "Cyclic Prefixing or Zero Padding for Wireless Multicarrier Transmissions?" *IEEE Transactions on Communications,*, vol. 50, pp. 2136–2148, Dec. 2002.

[7] MBOA-SIG, "Multiband OFDM Physical Layer Proposal for IEEE 802.15 Task Group 3a," *MultiBand OFDM Alliance SIG.*, Sep. 2004.

[8] J. G. Proakis, *Digital Communications*, 3rd ed. McGraw-Hill, 1995.

[9] "Channel Modeling Sub-committee Report (Final)," *IEEE 802.15 Working Group for Wireless Personal Area Networks(WPAN)*, Feb. 2003.